ACS APPLIED NANO MATERIALS

www.acsanm.org Article

Sonochemical Formation of Fluorouracil Nanoparticles: Toward Controlled Drug Delivery from Polymeric Surfaces

Paulina Chytrosz-Wrobel, Monika Golda-Cepa, Piotr Kubisiak, Waldemar Kulig, Lukasz Cwiklik,* and Andrzej Kotarba*

Cite This: *ACS Appl. Nano Mater.* 2023, 6, 4271−4278 Read Online

ACCESS | Metrics & More | Article Recommendations | Supporting Information

ABSTRACT: The biomaterial surface can be essentially upgraded with the therapeutic function by the introduction of controlled, local elution of biologically active molecules. The use of ultrasonic-assisted formation of nanoparticles with controlled size and morphology can be readily utilized for such functionalization. In this study, the synthesis route for the generation of nanoparticles of fluorouracil, the bioactive molecule used in anticancer therapy, was reported. The tandem of experimental (TEM, NTA, ATR-IR) and computational (MD simulations) approaches allowed us to obtain a molecular-level picture of the cavitation bubble interface where the enrichment of fluorouracil molecules takes place. Thanks to the originally developed computational model of cavitation bubbles, we revealed that the bubble interface plays a key role in the prearrangement of drug and solvent molecules, initiating the formation of nanoparticles' seeds. The proposed mechanism can be applied to other biologically relevant molecules, suggesting that the sonochemical method can be used for the controlled formation of their nanoparticles. The results indicate a feasible way to tailor the surface of polymeric biomaterials via the embedment of nanoparticles, thus having the potential to be used for practical implications as drug delivery systems.

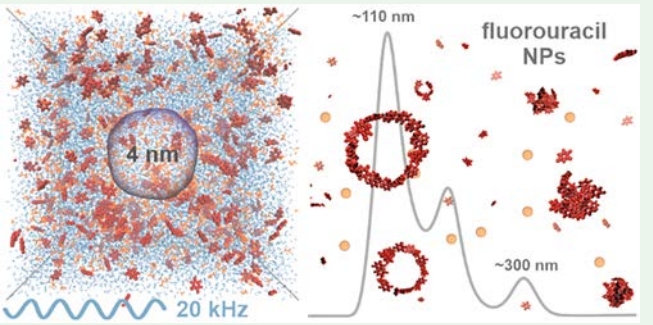

KEYWORDS: *drug nanoparticles, ultrasonic irradiation, cavitation bubble, nucleation mechanism, molecular dynamics*

INTRODUCTION

One of the areas of biointerface development dynamically advancing the most is implantable devices with therapeutic functions.[1] Owing to the combined work of engineers, chemists, physicists, biologists, and clinicians, the combination of nanotechnology and modern molecular medicine has led to increased interest in new drug delivery systems (DDS).[2−5] Therefore, the biomaterial surface can be substantially upgraded with the therapeutic function by the introduction of controlled, local elution of biologically active molecules (e.g., drugs, peptides, proteins).[6−8] The in-site release is one of the most rapidly developing areas of biomaterials engineering and offers numerous benefits when compared to conventional dosage forms (i.e., smaller doses of bioactive substances and minimal risk of side effects).[9,10] Ideally, biomaterials with a drug delivery function should enhance the therapeutic effect in the target place, reduce dosage and frequency, and thus accelerate recovery.[11] In particular, introducing the nanoparticles of bioactive molecules and controlling their surface dispersion and embedment in nanoscale have been brought to the forefront in DDS design and development. Nanosizing of drug crystallites increases their surface area and consequently promotes their dissolution rate and bioavailability, both of primary importance for pharmacokinetics.[12,13]

The use of ultrasound for formation of nanoparticles with controlled size and morphology has proved to be a simple, efficient, and eco-friendly method for compounds of varied chemical natures.[14−19] Despite the apparent advantages so far in the field of bioactive substances, only a few systems were successfully obtained via a sonochemical method: vitamin B12,[20] enzyme: amylase,[21] antibiotics: tetracycline,[22] and gentamicin.[23] The obtained nanoparticles of antibiotics were simultaneously deposited on a polymeric substrate forming DDS with elution for up to 7 days. Thus, it seems of particular importance to investigate other drug-polymer systems where the drug elution from the polymeric surface is advantageous, e.g., in anticancer therapy. One such system involves the improvement of polyurethane-based esophageal stents used in cancer palliative treatment.[24] For this application, fluorouracil is suggested as a systemic first-line drug. To limit its dose, fluorouracil nanoparticles can be sonochemically formed and

Received: December 15, 2022
Accepted: February 21, 2023
Published: March 1, 2023

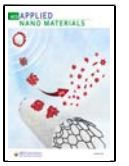

See https://pubs.acs.org/sharingguidelines for options on how to legitimately share published articles.

ACS Publications

© 2023 The Authors. Published by American Chemical Society

Scheme 1. Schematic Illustration of the Sonochemical Formation of Fluorouracil Nanoparticles and Their Application for Polymeric Drug Delivery Systems

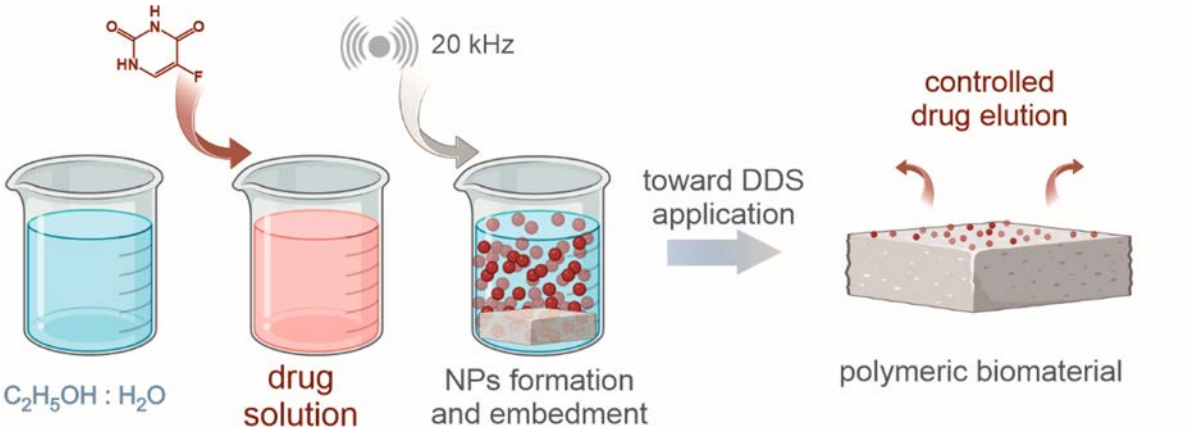

immobilized at the polyurethane cover of the stent and by prolonged elution act directly in the vicinity of the tumor.

The fundamental process that occurs when the solution is subjected to high-energy ultrasonic radiation is acoustic cavitation.[25] Sonochemical synthesis of nanoparticles is considered a complex process, where several steps are delineated. Initially, solutions are exposed to ultrasounds (in the range of 20 kHz−1 MHz), and the phenomenon of acoustic cavitation leads to bubble formation and growth. Once reaching a critical volume, the bubbles implode (their lifetime is ∼2 ns, and cooling rate is $\sim 10^{11}$ K/s),[26,27] and the dissolved molecules form nanoparticles. Due to the fast kinetics and molecular scale of the involved phenomena, the real-time experimental observations are problematic. Hence, the exact mechanism of the nanoparticles formation assisted by ultrasounds is still unknown, hindering further advancement in DDS based on the nanoparticles of bioactive molecules. Two possible mechanisms for the creation of sonochemical nanoparticles postulated so far are 1) solute molecules accumulate at the bubble interface, creating the shell of molecules,[22] which subsequently collapses and forms nanoparticles; and 2) nanoparticle seeds are preformed inside the cavitation bubble, initiating the particle growth.[28]

Molecular dynamics (MD) simulations have been widely used to study the details of biological processes occurring at biological interfaces.[29] They provide atomistic understanding of such processes and complement the experiments.[30] In the context of the sonochemistry of biological systems, MD simulations have successfully studied the bubble collapse and nanojet formation near a silica slab,[31] cavitation in water with a single nanoparticle embedded (silica),[32] and the ultrasound-driven collision between a pair of monoclinic zirconia NPs.[33]

At this stage, without a detailed understanding at the molecular level, further advancement in DDS based on the nanoparticles of bioactive molecules embedded into a polymeric surface is hindered. However, progress can be stimulated by utilizing computational methods for molecular modeling. In particular, the atomistic MD simulations can probe the short length and time scale while fully accounting for the dynamics and molecular complexity of the formation of sonochemical nanoparticles. In the broader perspective, with a fundamental understanding of this complex process, researchers will be able to design systems with targeted elution time and desired dosage, effectively reducing side effects.

In this study, a combination of experiments and atomistic MD simulations was employed to explore and optimize the mechanism of the sonochemically assisted formation of fluorouracil nanoparticles. The tandem of experimental and computational approaches allowed us to obtain a molecular-level picture of the cavitation bubble-solution interface where the fluorouracil drug molecules are present in a water/ethanol mixture. We revealed that such an interface plays a key role in the prearrangement of drug and solvent molecules, initiating the formation of nanoparticles seeds.

METHODS

Sonochemical Formation of Nanoparticles. A fluorouracil (Sigma-Aldrich) solution of 3 mg/mL was prepared by dissolving in deionized water and subsequently stirring for 15 min. To check the impact of solvent, the different active agent solutions were prepared containing the following ratios of ethanol to water: 10, 25, 50, and 75 wt.% deionized water (HydroLab, HLP 5), pure ethanol (99.8% POCH). The prepared solutions (3 mL) were then irradiated with homogenizer (Ti-horn, QSonica Q500) with the frequency of 20 kHz, amplitude 35%, pulse 2:1 (on:off), and time of 5 min. An ice bath was used to prevent overheating. The procedure is briefly summarized in Scheme 1.

Nanoparticles Tracking Analysis (NTA). The hydrodynamic diameters of sonochemically formed fluorouracil nanoparticles (FNPs) were determined using LM10 NanoSight instrument (Malvern Instruments Ltd.). The nanoparticles were illuminated with 450 nm blue laser, and then scattering was captured with sCMOS camera (Hamamatsu Photonics, Hamamatsu, Japan). Data were accumulated and analyzed with NTA software (3.1 Build 3.1.45). The Stokes−Einstein equation was used to calculate the mean hydrodynamic diameter. The size distribution was measured at camera level 15 (shutter: 1206, gain: 366). Analysis of each sample consisted of three movies, 30 s each at 25 frames/s.

ATR-IR. The stability of drug molecules under ultrasound waves was checked using the Attenuated Total Reflection Infrared Spectroscopy (ATR-IR). Spectra of fluorouracil and fluorouracil irradiated with ultrasounds were recorded using the Nicolet 6700 (Thermo Fisher Scientific) with diamond crystal. Each of the investigated samples was scanned 200 times in the range of 600−4000 cm^{-1}.

TEM. The TEM observations were carried out using an JEOL JEM2100 HT instrument operating at an accelerating voltage of 80 kV. The sonochemically prepared FNPs were taken immediately after the sonochemical formation from the solution and dropped on a Formvar film supported on a copper grid (Emgrid Australia).

MD Simulations. All MD simulations were carried out using the GROMACS 2020.5 software.[34] Force-field parameters of the

https://doi.org/10.1021/acsanm.2c05332
ACS Appl. Nano Mater. 2023, 6, 4271−4278

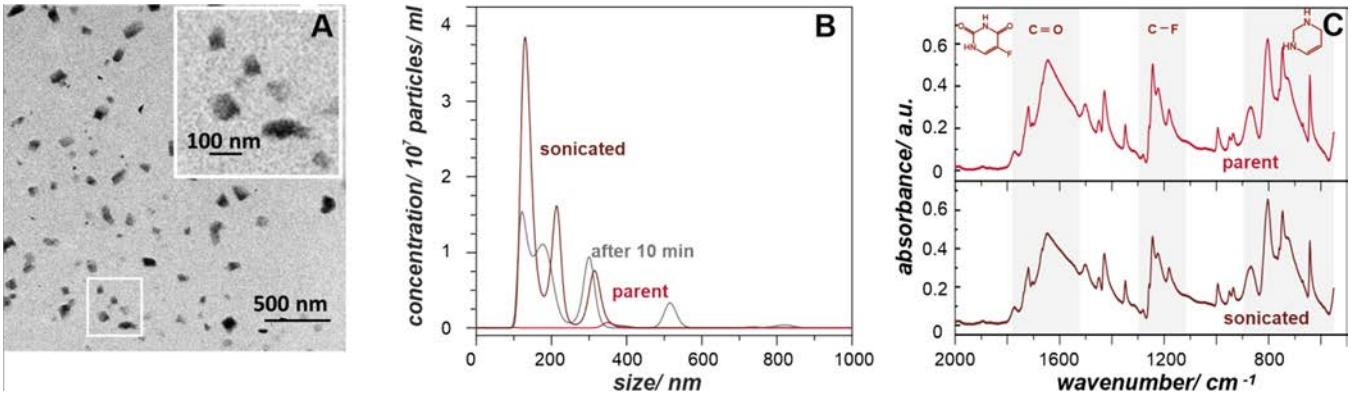

Figure 1. Physicochemical characterization of sonochemically formed nanoparticles of fluorouracil. (A) TEM image showing nanoparticles morphology, (B) NTA size distribution of formed NPs indicating their hydrodynamic diameters together with reference line (parent solution, before sonication) and 10 min after sonication, (C) ATR-IR spectra of the parent (untreated) fluorouracil (upper panel) and after its nanoparticles formation (lower panel), proving the intact molecular structure of the drug upon sonication.

Table 1. Detailed Compositions of *In Silico* Systems Used in MD Simulations

	solution			bubble−solution		
	water	ethanol	fluorouracil	water	ethanol	fluorouracil
water	50000	-	625	50000	-	625
mix10	48000	2000	625	48000	2000	625
mix25	44000	6000	625	44000	6000	625
mix50	36000	14000	625	36000	14000	625
mix75	23000	27000	625	23000	27000	625
ethanol	-	50000	625	-	50000	625

fluorouracil and ethanol molecules were taken from the Amber ff99SB-ILDN,[35] and the TIP3P water model[36] was used. Periodic boundary conditions were employed in all dimensions. After construction, all systems were energy-minimized using the steepest descent algorithm to remove close contacts. Then the 200 ps equilibration using NpT ensemble was performed, followed by production runs at the temperature of 310 K. The Nosé−Hoover thermostat,[37] with a time constant of 0.5 ps, was employed to keep the temperature constant. The Parrinello−Rahman barostat[38] was used to keep the pressure at 1 bar with a time constant of 10 ps. The production run length for all simulations was 100 ns and was repeated 3 times.

Covalent bonds were constrained by the LINCS algorithm[39] allowing for the 2 fs time step, while water molecules were kept constrained using the SETTLE method.[40] The long-range electrostatic interactions, calculated using the Particle Mesh Ewald algorithm,[41] were truncated at 1.4 nm. For the long-range nonbonded interactions, a 1.6 nm cutoff was used, and a 1.4 nm cutoff was employed for short-range interactions. Several measurable quantities have been extracted from the MD trajectories using the standard GROMACS tools and in-house scripts. VMD software[42] was used for visualization.

RESULTS AND DISCUSSION

Characterization of Sonochemically Obtained Fluorouracil Nanoparticles. The STEM images of sonochemically obtained fluorouracil NPs are presented in Figure 1A. The majority of the particles are in the narrow range of sizes from ∼80 to 120 nm. No evidence of macroparticles was found in the observed samples; however, aggregates of nanoparticles of ∼300 nm were also observed. The results of nanoparticle-tracking analysis for the sonochemically obtained fluorouracil nanoparticles are presented in Figure 1B. Whereas the NTA profile for the parent solution (before sonication) does not exhibit any maxima, for the sonicated solution the fluorouracil nanoparticles are observed. Immediately after the sonication, the profile is dominated by a maximum at ∼100 nm, followed by the less pronounced peaks at 200 and 300 nm, corresponding well to the sizes of the NPs in the TEM images (Figure 1A). Measurements performed postsonication process after a longer time revealed the agglomeration of the nanoparticles. This is illustrated by the representative results for 10 min, where the increase in maxima, for higher hydrodynamic diameters of the NPs (∼200, 300, 500 nm), is visible. These correspond to NPs agglomerates as their size is equal to multiples of diameters. It should be mentioned that the developed method for the synthesis of nanoparticles and their application for immediate deposition on the polymeric surface could be considered a one-step process (see Scheme 1). Therefore, in this case, the agglomeration kinetics is of secondary importance.

The ATR-IR spectra of the parent (upper panel) and sonicated (lower panel) fluorouracil are presented in Figure 1C. The recorded spectra show the characteristic C═O stretching band of fluorouracil at 1652 cm^{-1} and the sharp band at 1721 cm^{-1}, as well as the C−F stretching band at 1244 cm^{-1}.[43] In the low-frequency region of the spectra (<1000 cm^{-1}), in addition to the absorption bands of stretching vibrations of the pyrimidine ring and planar deformation vibrations, there are absorption bands of nonplanar deformation vibrations of fluorouracil.[44] The spectra exhibit an excellent agreement with the reference data and confirm the structural integrity of the fluorouracil molecules upon the ultrasonic treatment. These results have practical implications showing that all the functional groups of fluorouracil and its biological activity are preserved.

Computational Model of the Cavitation Bubble. MD simulations were employed to gain molecular insight into the

https://doi.org/10.1021/acsanm.2c05332
ACS Appl. Nano Mater. 2023, 6, 4271−4278

early stages of sonochemical formation of fluorouracil nanoparticles. We focused on studying the impact of solvent on this phenomenon; thus, the model systems with different ethanol concentrations in water (10 wt.%, 25 wt.%, 50 wt.%, and 75 wt.% ethanol in water, details about compositions are listed in Table 1) and fluorouracil were constructed with the use of Packmol package.[45] For every system, the number of fluorouracil molecules was fixed at 625. A total of 50,625 molecules were packed in the simulation box with the initial size of at least 12 × 12 × 12 nm. These systems correspond to the experimental bulk-solution conditions (see Figure 2A). The second group of *in silico* models contained the cavitation bubble. The spherical cavitation bubble (radius 2 nm) has been created in the middle of the cubic simulation box with a mixture of fluorouracil and solvents using the flat-bottomed position restraints. These systems are referred to as bubble-solvent systems in this work (see Figure 2B). The force constant of 1,000 kJ/(mol nm^2) has been used. The system was allowed to equilibrate for 100 ns, after which the restraints were removed leading to the collapse of the bubble (see bottom panel of Figure 2 and Movie S1).

Additionally, the reference systems (with corresponding amounts of fluorouracil, water, and ethanol) in the slab configuration containing the liquid–air interface have been created to check if the curvature of the bubble–solution interface influences the location and orientation of the fluorouracil molecules at the air–solution interface.

MD Insights into Sonochemical Formation of Fluorouracil Clusters. In Figure 3, the radial distribution function of fluorouracil molecules in ethanol–water solutions is presented. The orientation of fluorouracil molecules significantly differs between pure water and pure ethanol due to the different chemical nature of these solvents and mutual interactions between the solute and solvents. In the pure ethanol (dark brown curve in Figure 3), there is one dominant distance between the drug molecules around 0.65 nm, while in the pure water (dark blue curve in Figure 3), two possible orientations are observed with the intermolecular distance of ~0.45 and 0.60 nm. The number of molecules in both characteristic orientations depends on the ethanol to water ratio. Figure 3 provides the quantitative information on the changes induced by the addition of ethanol to fluorouracil–water systems. At 50 wt.% ethanol concentration, the average distance between fluorouracil molecules is longer (about 0.60 nm), and most of the drug molecules behave as in pure ethanol (orange-brown lines in Figure 3). On the other hand, at lower ethanol concentrations (mix10 and mix25, blue lines in Figure 3), the average distances between fluorouracil molecules are similar to that in pure water. The obtained profiles clearly illustrate that one can control the preferential fluorouracil arrangement by changing the ethanol to water ratio and, thus, stimulate the drug's nanoparticles formation.

Since the mix10 solution (10 wt.% ethanol in water) results in the most effective formation of fluorouracil nanoparticles, the molecular interactions were analyzed in detail for this system. To gain additional insight into the mutual orientation

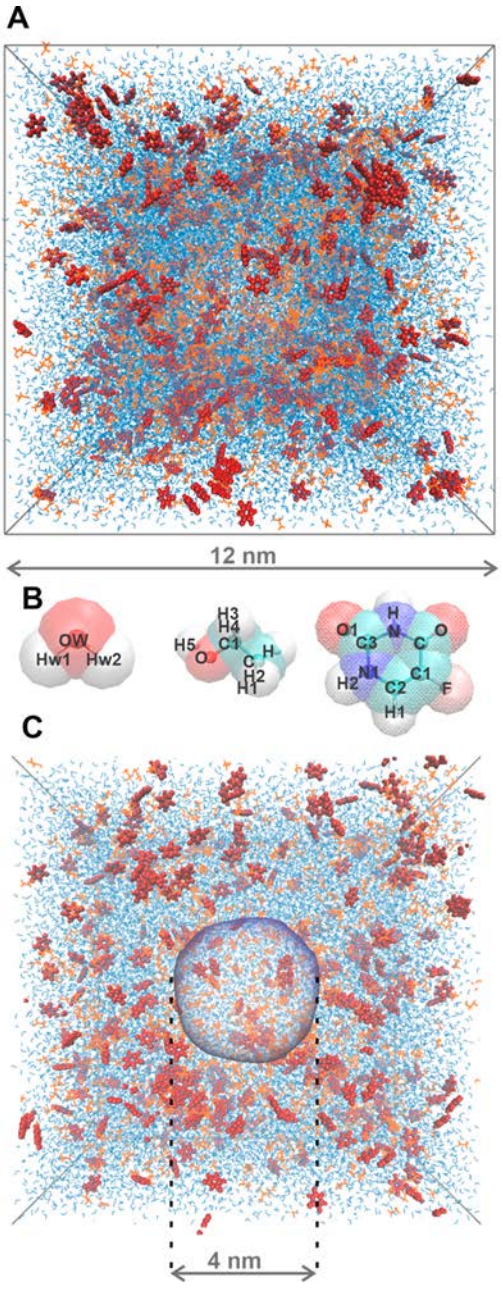

Figure 2. Snapshot of the simulation box showing (A) the system, (B) molecules with detailed atom names, and (C) cross section focusing on the bubble interface.

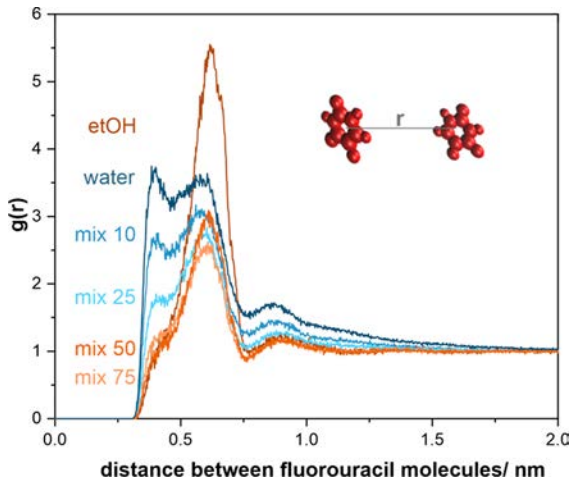

Figure 3. Fluorouracil–fluorouracil radial distribution functions (RDFs) in solutions with different ethanol-to-water ratios.

https://doi.org/10.1021/acsanm.2c05332
ACS Appl. Nano Mater. 2023, 6, 4271–4278

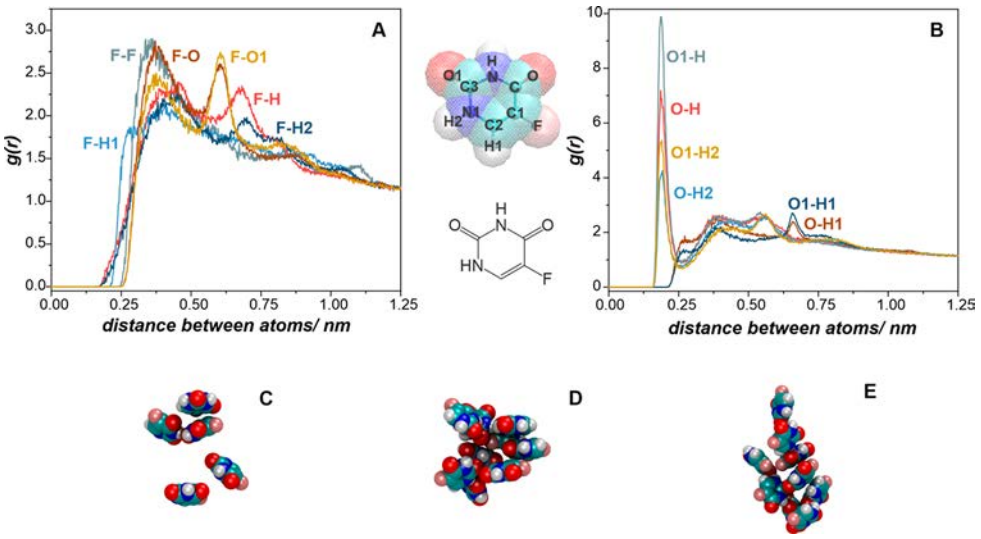

Figure 4. RDFs showing (A) the intermolecular fluorouracil binding preferences for fluorine and (B) oxygen atoms in the mix10 solution. Both fluorine and oxygen atoms show specific intermolecular binding preferences. Due to the dynamic nature of the formed clusters, assigning individual peaks to specific intermolecular cluster structures is difficult. The snapshots (C-E) show exemplary fluorouracil clusters (using 1 nm-distance criterion for clustering).

of fluorouracil in the solution, the RDFs of specific atom pairs in the fluorouracil have been calculated (Figure 4). The fluorouracil molecules seem to cluster together in a similar manner as benzene molecules ($\pi-\pi$ stacking). The maxima visible in the RDFs of F−F (at 0.35 nm) and F−O1 (at 0.60 nm) suggest that the preferred orientation of fluorouracil molecules in the fluorouracil clusters are such that the fluorouracil molecule is rotated either 0° or 180° with respect to its neighbor, as depicted by structures D and E in Figure 4. However, other orientations are also possible, e.g., structure C in Figure 4, where two fluorouracil molecules are rotated 90° with respect to each other, giving rise to other maxima in the RDFs.

In order to characterize the effect of the bubble−solution interface on the orientation of the fluorouracil, the RDFs of different chemical species as a function of the distance from the center of the bubble for the mix10 system have been calculated and depicted in Figure 5. Ethanol molecules clearly tend to locate at the bubble-solution interface, while water molecules avoid being exposed to a vacuum. Interestingly, fluorouracil locates in between the ethanol and water molecules and orients itself such that the fluorine atom points toward the bubble while the O1 atom points in the direction of the solution. The presence of the interface seems to facilitate the clustering and orienting of the fluorouracil molecules.

We also performed MD simulations mimicking a sonobubble collapse by removing the potential after 100 ns. Importantly, the simulated collapse did not result in the formation (see Figure 6) of large fluorouracil clusters in the collapsing bubble as previously suggested in previous research.[28] Thus, our molecular simulations support the key role of the bubble interface in the nanoparticles formation postulated in the literature.[22]

Mechanism of Sonochemical Formation of Fluorouracil Nanoparticles. The mechanism of the fluorouracil nanoparticles formation via the sonochemical method is schematically presented in Scheme 2 where the main steps of synthesis implied by the MD simulations and experiments are indicated: 1) starting from the initial solution of

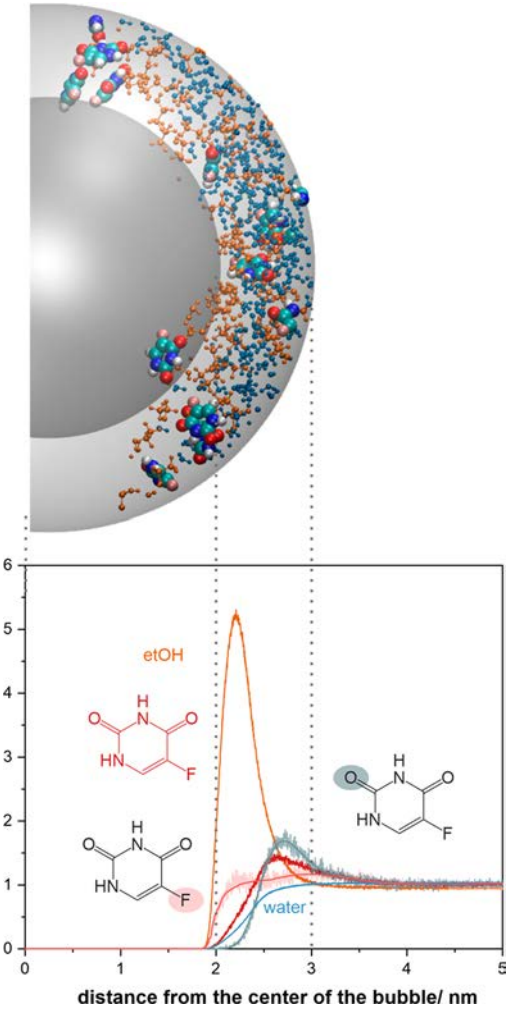

Figure 5. RDFs and the corresponding snapshot from the MD trajectory of the mix10 bubble-solution system. RDFs of two atoms (F and O1) of fluorouracil molecules (lower panel) were tracked to gain insight into its specific orientation at the bubble−solution interface.

https://doi.org/10.1021/acsanm.2c05332
ACS Appl. Nano Mater. 2023, 6, 4271−4278

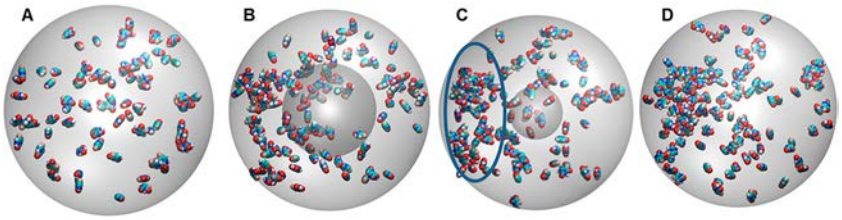

Figure 6. Main steps of fluorouracil seeds formation at the bubble−solution interface: (A) the initial mixture of fluorouracil, water, and ethanol; (B) the sonicated solution with cavitation bubble; (C) the collapsing cavitation bubble and the region of NP nucleation; (D) postcollapse aftergrowth of the drug particle.

Scheme 2. Mechanistic Scheme of the Sonochemical Formation of Fluorouracil Nanoparticles Emerging from the MD Simulations and Experimental Results

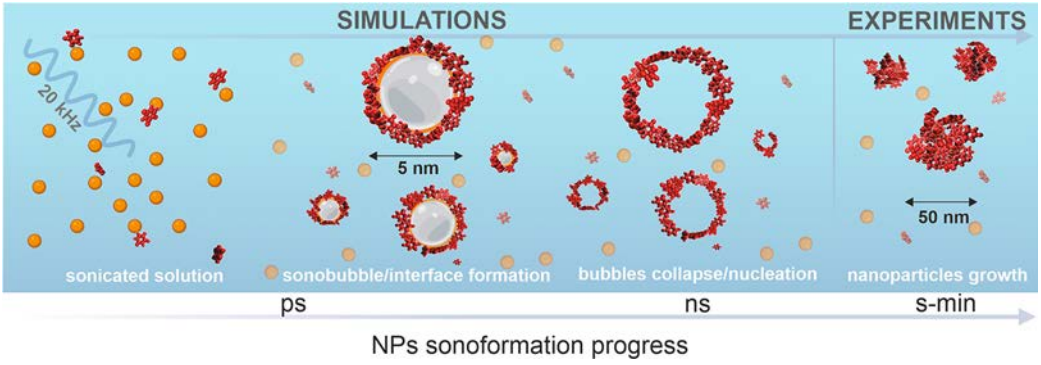

water−ethanol−fluorouracil (represented by the blue medium, orange balls, and red shapes, respectively), 2) passing through the formation of cavitation bubbles with the agglomeration of fluorouracil molecules at the interface, 3) the subsequent bubble collapsing, 4) eventually leading to the formation of the nucleation seeds, and 5) finally leading to the nanoparticles formation. The sonochemical irradiation stimulates the growth of the bubble since the excess of energy causes local evaporation of the solvent. After reaching the critical size, the bubble collapses since the interactions at the interface cannot sustain the phase boundary. The fluorouracil clusters formed at the interface are stable over time as observed experimentally. The further growth of nanoparticles is due to the fluorouracil crystallites' lattice energy of formation. The timeframes in Scheme 2 are provided for each step, which also determines the boundaries of simulation and experimental *modus operandi*. Taking into account that, in the same sonochemical process, the nanoparticles can be anchored at the polymeric surface (60 nm of gentamicin embedded into parylene C surface,[23] 100 nm fluorouracil embedded into parylene C and polyurethane in Figure S1 and S2, respectively), the results obtained here provide a suitable platform for functionalization of polymeric biomedical devices. Thus, at this stage of research, the proof of concept has been provided and, notably, the proposed approach can be easily extended to other bioactive molecules and polymeric materials.

CONCLUSIONS

In this study, we have successfully generated for the first time nanoparticles of fluorouracil, the bioactive molecule used in anticancer therapy. The formation of nanoparticles was stimulated by sonication of the fluorouracil−water−ethanol solution, while optimizing the irradiation parameters to keep the drug's molecular structure intact. The distribution of the formed nanoparticles was fairly homogeneous with an average size of ∼100 nm, which is a suitable size for controlled drug delivery. Fully atomistic molecular dynamics simulations were employed with a novel approach to model the cavitation bubbles and explain the mechanism of the formation of the nanoparticles at the molecular level. Combining experiments and computations can be used for the conceptualization of facile sonochemical synthesis of polymeric anticancer nanoparticle-based systems for the functionalization of esophageal stent covers. Such an approach is beneficial for the tunable, knowledge-based design, development, and optimization of therapeutic nanoparticles-based systems.

ASSOCIATED CONTENT

Supporting Information

The Supporting Information is available free of charge at https://pubs.acs.org/doi/10.1021/acsanm.2c05332.

Movie showing the fluorouracil clusters formation simulated in the mix10 solution (MP4)

Figures S1 and S2 depicting the ATR-IR spectra of parylene C and polyurethane surfaces decorated with fluorouracil NPs, respectively (PDF)

AUTHOR INFORMATION

Corresponding Authors

Lukasz Cwiklik − *J. Heyrovsky Institute of Physical Chemistry, Czech Academy of Sciences, 18223 Prague, Czech Republic; Institute of Organic Chemistry and Biochemistry of the Czech Academy of Sciences, CZ-16000 Prague 6, Czech Republic;* orcid.org/0000-0002-2083-8738; Email: lukasz.cwiklik@jh-inst.cas.cz

Andrzej Kotarba − *Faculty of Chemistry, Jagiellonian University in Krakow, 30-387 Krakow, Poland;* orcid.org/0000-0003-4815-0051; Email: kotarba@chemia.uj.edu.pl

https://doi.org/10.1021/acsanm.2c05332
ACS Appl. Nano Mater. 2023, 6, 4271−4278

Authors

Paulina Chytrosz-Wrobel − *Faculty of Chemistry, Jagiellonian University in Krakow, 30-387 Krakow, Poland;* orcid.org/0000-0002-9574-3151

Monika Golda-Cepa − *Faculty of Chemistry, Jagiellonian University in Krakow, 30-387 Krakow, Poland;* orcid.org/0000-0001-9054-4682

Piotr Kubisiak − *Faculty of Chemistry, Jagiellonian University in Krakow, 30-387 Krakow, Poland;* orcid.org/0000-0002-2680-2461

Waldemar Kulig − *Department of Physics, University of Helsinki, FI-00014 Helsinki, Finland;* orcid.org/0000-0001-7568-0029

Complete contact information is available at: https://pubs.acs.org/10.1021/acsanm.2c05332

Notes

The authors declare no competing financial interest.

■ ACKNOWLEDGMENTS

The authors thank the shared Czech-Polish research funding from the Czech Science Foundation (22-27317K) and NCN (2021/03/Y/ST4/00071). This research was supported, in part, by PLGrid Infrastructure (PLG/2021/014762, PLG/2021/014957, PLG/2022/015495). We wish to acknowledge the CSC − IT Center for Science (Espoo, Finland) for computational resources.

■ REFERENCES

(1) Han, X.; Alu, A.; Liu, H.; Shi, Y.; Wei, X.; Cai, L.; Wei, Y. Biomaterial-assisted biotherapy: A brief review of biomaterials used in drug delivery, vaccine development, gene therapy, and stem cell therapy Bioact. *Mater.* **2022**, *17*, 29−48.

(2) Kowalski, P. S.; Bhattacharya, C.; Afewerki, S.; Langer, R. Smart Biomaterials: Recent Advances and Future Directions. *ACS Biomater. Sci. Eng.* **2018**, *4* (11), 3809−3817.

(3) Patra, J. K.; Das, G.; Fraceto, L. F.; Campos, E. V. R.; Rodriguez-Torres, M. D. P.; Acosta-Torres, L. S.; Diaz-Torres, L. A.; Grillo, R.; Swamy, M. K.; Sharma, S.; Habtemariam, S.; Shin, H. S. Nano based drug delivery systems: recent developments and future prospects. *J. Nanobiotechnology* **2018**, *16* (1), 1−33.

(4) Wang, Y.; Chen, G.; Zhang, H.; Zhao, C.; Sun, L.; Zhao, Y. Emerging Functional Biomaterials as Medical Patches. *ACS Nano* **2021**, *15* (4), 5977−6007.

(5) Han, Y.; Shchukin, D.; Yang, J.; Simon, C. R.; Fuchs, H.; Möhwald, H. Biocompatible protein nanocontainers for controlled drugs release. *ACS Nano* **2010**, *4* (5), 2838−2844.

(6) Zhang, Q.; Zhang, J.; Song, J.; Liu, Y.; Ren, X.; Zhao, Y. Protein-Based Nanomedicine for Therapeutic Benefits of Cancer. *ACS Nano* **2021**, *15* (5), 8001−8038.

(7) Qin, S. Y.; Zhang, A. Q.; Cheng, S. X.; Rong, L.; Zhang, X. Z. Drug self-delivery systems for cancer therapy Biomaterials. *Biomaterials* **2017**, *112*, 234−247.

(8) Martin, V.; Bettencourt, A. A. Bone regeneration: Biomaterials as local delivery systems with improved osteoinductive properties Mater. *Sci. Eng. C* **2018**, *82*, 363−371.

(9) Bajpai, S.; Tiwary, S. K.; Sonker, M.; Joshi, A.; Gupta, V.; Kumar, Y.; Shreyash, N.; Biswas, S. Recent Advances in Nanoparticle-Based Cancer Treatment: A Review. *ACS Appl. Nano Mater.* **2021**, *4* (7), 6441−6470.

(10) Kumar, R.; Dalvi, S. V.; Siril, P. F. Nanoparticle-Based Drugs and Formulations: Current Status and Emerging Applications. *ACS Appl. Nano Mater.* **2020**, *3* (6), 4944−4961.

(11) Fenton, O. S.; Olafson, K. N.; Pillai, P. S.; Mitchell, M. J.; Langer, R. Advances in Biomaterials for Drug Delivery. *Adv. Mater.* **2018**, *30* (29), 1705328.

(12) Verma, V.; Ryan, K. M.; Padrela, L. *Production and isolation of pharmaceutical drug nanoparticles International Journal of Pharmaceutics* **2021**, *603*, 120708.

(13) Al-Kassas, R.; Bansal, M.; Shaw. Nanosizing techniques for improving bioavailability of drugs. *J. Journal of Controlled Release* **2017**, *260*, 202−212.

(14) Bang, J. H.; Suslick, K. S. Applications of Ultrasound to the Synthesis of Nanostructured Materials. *Adv. Mater.* **2010**, *22* (10), 1039−1059.

(15) Pokhrel, N.; Vabbina, P. K.; Pala, N. Sonochemistry: Science and Engineering. *Ultrasonics Sonochemistry* **2016**, *29*, 104−128.

(16) Liu, X.; Wu, Z.; Cavalli, R.; Cravotto, G. Preparation of Inorganic Nanoparticles and Nanocomposites for Drug Release-A Review. *Ind. Eng. Chem. Res.* **2021**, *60* (28), 10011−10032.

(17) Fuentes-García, J. A.; Santoyo-Salzar, J.; Rangel-Cortes, E.; Goya, G. F.; Cardozo-Mata, V.; Pescador-Rojas, J. A. Effect of ultrasonic irradiation power on sonochemical synthesis of gold nanoparticles Ultrason. *Sonochem* **2021**, *70*, 105274.

(18) Iline-Vul, T.; Bretler, S.; Cohen, S.; Perelshtein, I.; Perkas, N.; Gedanken, A.; Margel, S. Engineering of superhydrophobic silica microparticles and thin coatings on polymeric films by ultrasound irradiation Mater. *Today Chem.* **2021**, *21*, 100520.

(19) Rogowska-Tylman, J.; Locs, J.; Salma, I.; Woźniak, B.; Pilmane, M.; Zalite, V.; Wojnarowicz, J.; Kędzierska-Sar, A.; Chudoba, T.; Szlązak, K.; Chlanda, A.; Święszkowski, W.; Gedanken, A.; Łojkowski, W. In vivo and in vitro study of a novel nanohydroxyapatite sonocoated scaffolds for enhanced bone regeneration Mater. *Sci. Eng. C* **2019**, *99*, 669−684.

(20) Fixler, D.; Yariv, I.; Lipovsky, A.; Gedanken, A.; Lubart, R. Enhanced pharmacological activity of Vitamin B12 and Penicillin as nanoparticles. *Int. J. Nanomedicine* **2015**, *10* (1), 3593.

(21) Meridor, D.; Gedanken, A. Preparation of enzyme nanoparticles and studying the catalytic activity of the immobilized nanoparticles on polyethylene films Ultrason. *Sonochem* **2013**, *20* (1), 425−431.

(22) Grinberg, O.; Natan, M.; Lipovsky, A.; Varvak, A.; Keppner, H.; Gedanken, A.; Banin, E. Antibiotic nanoparticles embedded into the Parylene C layer as a new method to prevent medical device-associated infections. *J. Mater. Chem. B* **2015**, *3* (1), 59−64.

(23) Golda-Cepa, M.; Chytrosz, P.; Chorylek, A.; Kotarba, A. One-step sonochemical fabrication and embedding of gentamicin nanoparticles into parylene C implant coating: towards controlled drug delivery Nanomedicine Nanotechnology. *Biol. Med.* **2018**, *14* (3), 941−950.

(24) Chytrosz, P.; Golda-Cepa, M.; Wlodarczyk, J.; Kuzdzal, J.; El Fray, M.; Kotarba, A. Characterization of Partially Covered Self-Expandable Metallic Stents for Esophageal Cancer Treatment: In Vivo Degradation. *ACS Biomater. Sci. Eng.* **2021**, *7* (4), 1403−1413.

(25) Suslick, K. S.; Eddingsaas, N. C.; Flannigan, D. J.; Hopkins, S. D.; Xu, H. The Chemical History of a Bubble. *Acc. Chem. Res.* **2018**, *51* (9), 2169−2178.

(26) Hinman, J. J.; Suslick, K. S. Nanostructured Materials Synthesis Using Ultrasound. *Topics in Current Chemistry* **2017**, *375*, 12.

(27) Gedanken, A. Doping nanoparticles into polymers and ceramics using ultrasound radiation Ultrason. *Sonochem* **2007**, *14* (4), 418−430.

(28) Xu, H.; Zeiger, B. W.; Suslick, K. S. Sonochemical synthesis of nanomaterials. *Chem. Soc. Rev.* **2013**, *42* (7), 2555−2567.

(29) Enkavi, G.; Javanainen, M.; Kulig, W.; Róg, T.; Vattulainen, I. Multiscale Simulations of Biological Membranes: The Challenge To Understand Biological Phenomena in a Living Substance. *Chem. Rev.* **2019**, *119* (9), 5607−5774.

(30) Gupta, K. M.; Das, S.; Chow, P. S.; Macbeath, C. Encapsulation of Ferulic Acid in Lipid Nanoparticles as Antioxidant for Skin: Mechanistic Understanding through Experiment and Molecular Simulation ACS Appl. *Nano Mater.* **2020**, *3* (6), 5351−5361.

(31) Shekhar, A.; Nomura, K. I.; Kalia, R. K.; Nakano, A.; Vashishta, P. Nanobubble collapse on a silica surface in water: Billion-atom

reactive molecular dynamics simulations. *Phys. Rev. Lett.* **2013**, *111* (18), 184503.
(32) Li, B.; Gu, Y.; Chen, M. Cavitation inception of water with solid nanoparticles: A molecular dynamics study Ultrason. *Sonochem* **2019**, *51*, 120−128.
(33) Yao, Z.; Zhang, H.; Hu, Y.; Bian, J.; Wang, G.; Lu, J.; Niu, X. Ultrasound driven aggregation—A novel method to assemble ceramic nanoparticles Extrem. *Mech. Lett.* **2016**, *7*, 71−77.
(34) Abraham, M. J.; Murtola, T.; Schulz, R.; Páll, S.; Smith, J. C.; Hess, B.; Lindahl, E. GROMACS: High performance molecular simulations through multi-level parallelism from laptops to supercomputers. *SoftwareX* **2015**, *1−2*, 19−25.
(35) Lindorff-Larsen, K.; Piana, S.; Palmo, K.; Maragakis, P.; Klepeis, J. L.; Dror, R. O.; Shaw, D. E. Improved side-chain torsion potentials for the Amber ff99SB protein force field Proteins. *Struct. Funct. Bioinforma.* **2010**, *78* (8), 1950−1958.
(36) Chen, F.; Smith, P. E. Simulated surface tensions of common water models. *J. Chem. Phys.* **2007**, *126* (22), 221101.
(37) Nosé, S. A molecular dynamics method for simulations in the canonical ensemble. *Molecular physics* **1984**, *52* (2), 255−268.
(38) Bussi, G.; Donadio, D.; Parrinello, M. Canonical sampling through velocity rescaling. *J. Chem. Phys.* **2007**, *126* (1), 014101.
(39) Hess, B.; Bekker, H.; Berendsen, H. J. C.; Fraaije, J. G. E. M. LINCS: A Linear Constraint Solver for Molecular Simulations. *J. Comput. Chem.* **1997**, *18*, 1463−1472.
(40) Hockney, R. W.; Goel, S. P.; Eastwood, J. W. Quiet high-resolution computer models of a plasma. *J. Comput. Phys.* **1974**, *14* (2), 148−158.
(41) Essmann, U.; Perera, L.; Berkowitz, M. L.; Darden, T.; Lee, H.; Pedersen, L. G. A smooth particle mesh Ewald method. *J. Chem. Phys.* **1995**, *103* (19), 8577.
(42) Humphrey, W.; Dalke, A.; Schulten, K. VMD: Visual molecular dynamics. *J. Mol. Graph.* **1996**, *14* (1), 33−38.
(43) Melnikova, D. L.; Badrieva, Z. F.; Kostin, M. A.; Maller, C.; Stas, M.; Buczek, A.; Broda, M. A.; Kupka, T.; Kelterer, A. M.; Tolstoy, P. M.; Skirda, V. D. On Complex Formation between 5-Fluorouracil and β-Cyclodextrin in Solution and in the Solid State: IR Markers and Detection of Short-Lived Complexes by Diffusion. *NMR Mol.* **2020**, *25* (23), 5706.
(44) Ivanov, A. Y.; Leontiev, V. S.; Belous, L. F.; Rubin, Y. V.; Karachevtsev, V. A. Infrared spectra of 5-fluorouracil molecules isolated in inert Ar matrices, and their films on graphene oxide at 6 K Low Temp. *Phys.* **2017**, *43* (3), 400.
(45) Martinez, L.; Andrade, R.; Birgin, E. G.; Martínez, J. M. PACKMOL: a package for building initial configurations for molecular dynamics simulations. *J. Comput. Chem.* **2009**, *30* (13), 2157−2164.

https://doi.org/10.1021/acsanm.2c05332
ACS Appl. Nano Mater. 2023, 6, 4271−4278